Simple lattice Boltzmann model for simulating flows with shock wave

Yan Guangwu,[1,2,*] Chen Yaosong,[3] and Hu Shouxin[2]
[1]*Laboratory for Nonlinear Mechanics of Continuous Media, Institute of Mechanics, Chinese Academy of Sciences, Beijing 100080, China*
[2]*Department of Mathematics, Jilin University, Changchun 130023, China*
[3]*Department of Mechanics, Peking University, Beijing 100871, China*
(Received 20 January 1998; revised manuscript received 10 September 1998)

We propose a lattice Boltzmann model for compressible Euler equations. The numerical examples show that the model can be used to simulate shock wave and contact discontinuity. The results are compared with those obtained by traditional methods. [S1063-651X(98)13012-X]

PACS number(s): 47.10.+g

I. INTRODUCTION

In recent years, the lattice Boltzmann method (LBM) has developed into an alternative and promising numerical scheme for simulating fluid flows and modeling physics in fluids. Unlike traditional numerical methods which solve equations for macroscopic variables, the LBM is based on the mesoscopic kinetic equation for the particle distribution function. The fundamental idea of the LBM is to construct a simplified kinetic model that incorporates the essential physics of microscopic or mesoscopic processes and the macroscopic variables, and obeys the desired macroscopic equations [1]. The kinetic nature of the LBM has three important features that distinguish it from other numerical methods. First, the convection operator of the LBM is linear. Second, the incompressible Navier-Stokes equations can be obtained in the incompressible limit. Third, the LBM uses a minimal set of velocities. Since only a few moving directions are used, if we fix the direction, say α, the lattice Boltzmann equation is a one-dimensional iteration, and the code is greatly simplified.

As important progress, the simple collision model of Bhatnagar-Gross-Krook (BGK) was applied to the lattice Boltzmann equation, yielding the lattice BGK model [2–4]. However, this method is limited to a range of low Mach number as an image gas [5,6]. This is due to the following two reasons. (i) There exist nonlinear deviations, i.e., $\partial^2 \rho u_i u_j u_k / \partial x_j \partial x_k$. (ii) In the momentum equation there is a compressible factor $D_{ij} = (\partial/\partial x_j)\,\eta[u_i \partial\rho/\partial x_j + u_j \partial\rho/\partial x_i + \delta_{ij} u_k \partial\rho/\partial x_k + \frac{5}{3}\rho\delta_{ij}\partial u_k/\partial x_k]$ (see Ref. [6]).

It is a challenge to use pure lattice Boltzmann method to simulate the compressible Euler equations, especially for the problems which contain shock waves and contact discontinuities. Recently, there are some studies on the compressible flows, but the results are only for the situations of weak compressible and isothermal flows [4,5].

In this paper, using a square lattice, we will propose a three-speed-three-energy-level lattice Boltzmann model for a compressible perfect gas. This model is based on the following ideas [7].

(1) The fundamental framework and method are the same as those used in the standard LBM.

(2) The particles moving along every link are separated into two kinds with two different energy levels, and the rest particle possesses another energy level.

(3) Besides the conservation conditions of mass, momentum, and energy, the equilibrium distribution must satisfy the flux conditions of momentum and energy.

(4) In this model one can choose the speed of moving particles.

Numerical results show that this model works quite well for the simulation of strong discontinuity phenomena.

In Sec. II of this paper, based on a square lattice, a lattice Boltzmann model will be proposed. In Sec. III three famous test problems are calculated to examine this model. The results are satisfying.

II. LATTICE BOLTZMANN MODEL FOR COMPRESSIBLE EULER EQUATIONS

We use a square lattice with eight links that connects the center site to eight nearest neighbor nodes, that is, four face centers and four vertices (Fig. 1). We assume that the particles moving along the link with velocity $\mathbf{e}_\alpha$ are divided into two kinds, A and B, with two different energy levels $\varepsilon_A(\alpha = 1,...,8)$ and $\varepsilon_B(\alpha = 9,...,16)$, and the rest particle $(\alpha = 0)$ possesses energy level ε_D. So it is actually a 17-bit model with three speeds $0, c, \sqrt{2}c$, where c is the speed of particles at the face centers.

The following identities of velocity moments are necessary for the derivation of the model [8]:

$$\sum_\alpha e_{\alpha i} e_{\alpha j} = \begin{cases} bc^2\delta_{ij}/D & (\alpha = 1,3,5,7 \text{ or } 9,11,13,15) \\ 2bc^2\delta_{ij}/D & (\alpha = 2,4,6,8 \text{ or } 10,12,14,16), \end{cases} \tag{1}$$

$$\sum_\alpha e_{\alpha i} e_{\alpha j} e_{\alpha k} e_{\alpha m} = \begin{cases} 2c^4\delta_{ijkm} & (\alpha = 1,3,5,7 \text{ or } 9,11,13,15) \\ 4c^4\Delta_{ijkm} - 8c^4\delta_{ijkm} & (\alpha = 2,4,6,8 \text{ or } 10,12,14,16), \end{cases} \tag{2}$$

*Present address: Department of Mathematics, Jilin University, Changchun 130023, China.

where $b=4$, D is the space dimension, $\delta_{ijkm}=1$ if $i=j=k=m$, otherwise $\delta_{ijkm}=0$, $\Delta_{ijkm}=(\delta_{ij}\delta_{km}+\delta_{ik}\delta_{jm}+\delta_{im}\delta_{jk})$.

(1) The definition of the macroscopic variables. The single particle distribution in the ''shooting-in'' state at site $\mathbf{x}$ and time t is denoted by $f_\alpha=f_\alpha(\mathbf{x},t)$ $(\alpha=0,...,16)$. The mass, momentum, and total energy per site are defined as

$$\rho=\sum_\alpha f_\alpha, \tag{3}$$

$$\rho u_i=\sum_\alpha f_\alpha e_{\alpha i} \quad (i=1,2), \tag{4}$$

$$\tfrac{1}{2}\rho u^2+\rho E=\sum_\alpha f_\alpha \varepsilon_\alpha \quad (\varepsilon_\alpha=\varepsilon_A,\varepsilon_B,\varepsilon_D), \tag{5}$$

where E is the internal energy per unit mass.

(2) The updating rule of particle distribution. According to Refs. [2,3], the distribution f'_α of the ''shooting-out'' state after collisions is determined by the BGK-type lattice Boltzmann equation

$$f'_\alpha=f_\alpha-\frac{1}{\tau}(f_\alpha-f_\alpha^{\rm eq}) \quad (\alpha=0,...,16), \tag{6}$$

$$f_\alpha(\mathbf{x}+\mathbf{e}_\alpha\Delta t,t+\Delta t)=f'_\alpha(\mathbf{x},t), \tag{7}$$

where τ is the single relaxation time, and $f_\alpha^{\rm eq}$ is the local equilibrium distribution. Equations (6) and (7) are actually a finite-difference scheme which is not for macroscopic variables $\rho,\rho u_i,E$ but for ''mesoscopic'' variables f_α.

(3) Equilibrium distribution. We assume that the equilibrium distributions $f_\alpha^{\rm eq}$ in Eq. (6) have the same expressions as those in Refs. [2, 3],

$$f_0^{\rm eq}=D_0\rho+D_3\rho u^2,$$

$$f_\alpha^{\rm eq}=A_0^+\rho+A_1^+\rho u_i e_{\alpha i}+A_2^+\rho u_i u_j e_{\alpha i}e_{\alpha j}+A_3^+\rho u^2 \quad (\alpha=1,3,5,7),$$

$$f_\alpha^{\rm eq}=A_0^\times\rho+A_1^\times\rho u_i e_{\alpha i}+A_2^\times\rho u_i u_j e_{\alpha i}e_{\alpha j}+A_3^\times\rho u^2 \quad (\alpha=2,4,6,8), \tag{8}$$

$$f_\alpha^{\rm eq}=B_0^+\rho+B_1^+\rho u_i e_{\alpha i}+B_2^+\rho u_i u_j e_{\alpha i}e_{\alpha j}+B_3^+\rho u^2 \quad (\alpha=9,11,13,15),$$

$$f_\alpha^{\rm eq}=B_0^\times\rho+B_1^\times\rho u_i e_{\alpha i}+B_2^\times\rho u_i u_j e_{\alpha i}e_{\alpha j}+B_3^\times\rho u^2 \quad (\alpha=10,12,14,16),$$

where the symbols $+$, $\times$ mean odd and even direction number α. Here, coefficients $A_i^+,B_i^+,A_i^\times,B_i^\times,D_0,D_3$ are determined by a set of reasonable requirements. These requirements consist of the conservation laws of mass, momentum, energy, and the flux conditions of momentum and energy:

$$\sum_\alpha f_\alpha^{\rm eq}=\rho, \tag{9}$$

$$\sum_\alpha f_\alpha^{\rm eq}e_{\alpha i}=\rho u_i, \tag{10}$$

$$\sum_\alpha f_\alpha^{\rm eq}\varepsilon_\alpha=\tfrac{1}{2}\rho u^2+\rho E, \tag{11}$$

$$\sum_\alpha f_\alpha^{\rm eq}e_{\alpha i}e_{\alpha j}=\rho u_i u_j+p\,\delta_{ij}, \tag{12}$$

$$\sum_\alpha f_\alpha^{\rm eq}\varepsilon_\alpha e_{\alpha i}=(\tfrac{1}{2}\rho u^2+\rho E+p)u_i, \tag{13}$$

where p is the pressure of the perfect gas,

$$p=(\gamma-1)\rho E. \tag{14}$$

Substituting Eq. (8) into Eqs. (9)–(13) and using the identity (1) and (2), we obtain the system of linear equations for determining these coefficients,

$$D_0+b(A_0^++B_0^++A_0^\times+B_0^\times)=1, \tag{15}$$

$$\frac{bc^2}{D}[A_0^++B_0^++2(A_0^\times+B_0^\times)]=(\gamma-1)E, \tag{16}$$

$$\varepsilon_D D_0+b\varepsilon_A(A_0^++A_0^\times)+b\varepsilon_B(B_0^++B_0^\times)=E, \tag{17}$$

$$\frac{bc^2}{D}[A_1^++B_1^++2(A_1^\times+B_1^\times)]=1, \tag{18}$$

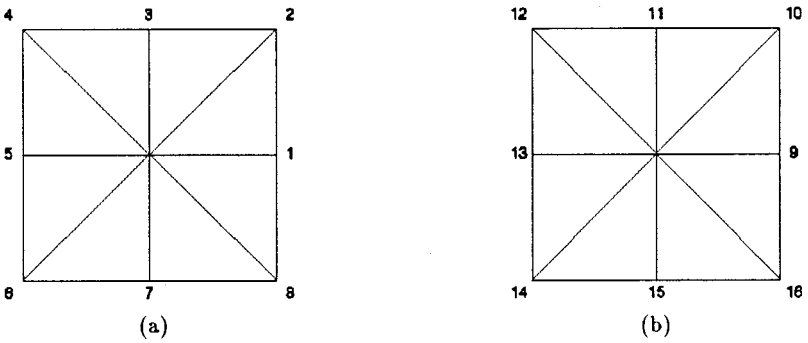

FIG. 1. A square lattice of the 17-bit model, (a) type *A*, (b) type *B*.

$$\frac{bc^2}{D}[\varepsilon_A A_1^+ + \varepsilon_B B_1^+ + 2(\varepsilon_A A_1^\times + \varepsilon_B B_1^\times)] = \tfrac{1}{2}u^2 + \gamma E, \tag{19}$$

$$A_2^+ + B_2^+ = 4(A_2^\times + B_2^\times), \tag{20}$$

$$A_2^\times + B_2^\times = 1/8c^4, \tag{21}$$

$$\frac{bc^2}{D}[A_3^+ + B_3^+ + 2(A_3^\times + B_3^\times)] + 4c^2(A_2^\times + B_2^\times) = 0, \tag{22}$$

$$D_3 + b(A_3^+ + B_3^+ + A_3^\times + B_3^\times) + [(A_2^+ + B_2^+) + 2(A_2^\times + B_2^\times)]bc^2/D = 0, \tag{23}$$

$$\varepsilon_0 D_3 + b\varepsilon_A(A_3^+ + A_3^\times) + b\varepsilon_B(B_3^+ + B_3^\times) + \frac{bc^2}{D}[\varepsilon_A A_2^+ + \varepsilon_B B_2^+ + 2(\varepsilon_A A_2^\times + \varepsilon_B B_2^\times)] = \frac{1}{2}. \tag{24}$$

First, if the requirements are reasonable, the system of equations should be consistent. Second, if the system has more unknowns than equations, as we see in Eqs. (15)–(24), we have to propose some man-made complementary conditions. We introduce an assumption to eliminate the coefficients $A_i^\times, B_i^\times$ to get a system of equations with unknowns A_i^+, B_i^+. Using a simpler method, we let

$$A_i^\times = A_i^+, \quad B_i^\times = B_i^+ \quad (i = 0,1,3), \tag{25}$$

$$A_2^\times = \tfrac{1}{4}A_2^+, \tag{26}$$

$$\varepsilon_A + A_2^+ + \varepsilon_B B_2^+ = \lambda \frac{2D}{3bc^2}. \tag{27}$$

Here, λ is a chosen parameter, called the separating factor, which may be taken as a contribution of each type particle to $f_\alpha^{(\mathrm{eq})}$ (or per energy level). If $\varepsilon_A = \varepsilon_B = \overline{\varepsilon}$, then this model becomes a standard lattice Boltzmann model (9-bit model), then $\lambda = 3b\overline{\varepsilon}/4Dc^2$. If $\varepsilon_A \neq \varepsilon_B$, then the meaning of λ is the coefficient of the equilibrium distribution by modifying the energy levels. Therefore all coefficients can be solved easily. Inserting the expressions of coefficients $A_i^+, A_i^\times, B_i^+, B_i^\times, D_i$ into Eq. (8), we can obtain the final form of equilibrium distribution.

Choosing time step Δt as small perturbation parameter ε, which plays the role of the Knudsen number [8], we use the multiscale technique and Chapman-Enskog expansion

$$\frac{\partial}{\partial t} = \frac{\partial}{\partial t_0} + \varepsilon \frac{\partial}{\partial t_1} + \varepsilon^2 \frac{\partial}{\partial t_2} + \cdots, \tag{28}$$

$$f_\alpha = f_\alpha^{\mathrm{eq}} + \varepsilon f_\alpha^{(1)} + \varepsilon^2 f_\alpha^{(2)} + \cdots. \tag{29}$$

Then the macroscopic dynamics equations of mass, momentum, and energy can be derived from the scheme (6)–(8). The leading order terms are the Euler equations of perfect gas with the truncation errors $R_i = O(\varepsilon)$.

$$\frac{\partial \rho}{\partial t} + \frac{\partial \rho u_i}{\partial x_i} = R_1 + O(\varepsilon^2), \tag{30}$$

$$\frac{\partial \rho u_i}{\partial t} + \frac{\partial \rho u_i u_j}{\partial x_j} + \frac{\partial p}{\partial x_j}\delta_{ij} = R_2 + O(\varepsilon^2), \tag{31}$$

$$\frac{\partial}{\partial t}\left(\frac{1}{2}\rho u^2 + \rho E\right) + \frac{\partial}{\partial x_i}\left(\frac{1}{2}\rho u^2 + \rho E + p\right)u_i = R_3 + O(\varepsilon^2), \tag{32}$$

where

$$R_1 = 0, \tag{33}$$

$$R_2 = \varepsilon\left(\tau - \frac{1}{2}\right)\left(\frac{\partial^2 \pi_{ij}^{(0)}}{\partial t_0 \partial x_j} + \frac{\partial^2 P_{ijk}^{(0)}}{\partial x_j \partial x_k}\right), \tag{34}$$

$$R_3 = \varepsilon\left(\tau - \frac{1}{2}\right)\left(\frac{\partial^2 Q_j^{(0)}}{\partial t_0 \partial x_j} + \frac{\partial^2 R_{jk}^{(0)}}{\partial x_j \partial x_k}\right), \tag{35}$$

where $\pi_{ij}^{(0)} = \Sigma_\alpha f_\alpha^{\mathrm{eq}} e_{\alpha i} e_{\alpha j}$, $Q_j^{(0)} = \Sigma_\alpha f_\alpha^{\mathrm{eq}} \varepsilon_\alpha e_{\alpha j}$, $P_{ijk}^{(0)} = \Sigma_\alpha f_\alpha^{\mathrm{eq}} e_{\alpha i} e_{\alpha j} e_{\alpha k}$, $R_{ij}^{(0)} = \Sigma_\alpha f_\alpha^{\mathrm{eq}} \varepsilon_\alpha e_{\alpha i} e_{\alpha j}$. This scheme has the first order accuracy of the truncation errors [9].

III. NUMERICAL EXAMPLES

In this section three famous test problems are calculated to examine the performance of this model in the simulation of aerodynamics.

Example (1). The Sod test [10] which consists of initial data on the left and right side,

$$(\rho_L, u_L, p_L) = (1,0,1), \quad x < 0$$

$$(\rho_R, u_R, p_R) = (0.125,0,0.1), \quad x > 0.$$

Example (2). The Lax test [11] with initial data

$$(\rho_L, u_L, p_L) = (0.445,0.698,3.528), \quad x < 0,$$

$$(\rho_R, u_R, p_R) = (0.5,0,0.571) \quad x > 0.$$

The comparisons between numerical and exact results are plotted in Fig. 2 (for Sod's test) and Fig. 3 (for Lax's test). They show the formation of shock waves, contact discontinuities, and rarefaction waves. The widths of shock waves are about three to four cells, the speed of shock waves coincides with the theoretical predication. To sum up, the numerical results are well consistent with the theoretical ones. However, on the pressure profiles on the position corresponding to the contact discontinuities, we also found some obvious errors which are not dissipation or dispersion. This kind of errors has been found in some traditional schemes such as in Ref. [12]. Table I shows the L_1 norm errors in our lattice Boltzmann model and other schemes. Another problem is that the ''platform'' between shock wave and contact discontinuity in the Lax problem emerges quite late.

Example (3). The Roe test [13] with the following initial data:

$$(\rho_L, u_L, p_L) = (1,-1,1.8), \quad x < 0$$

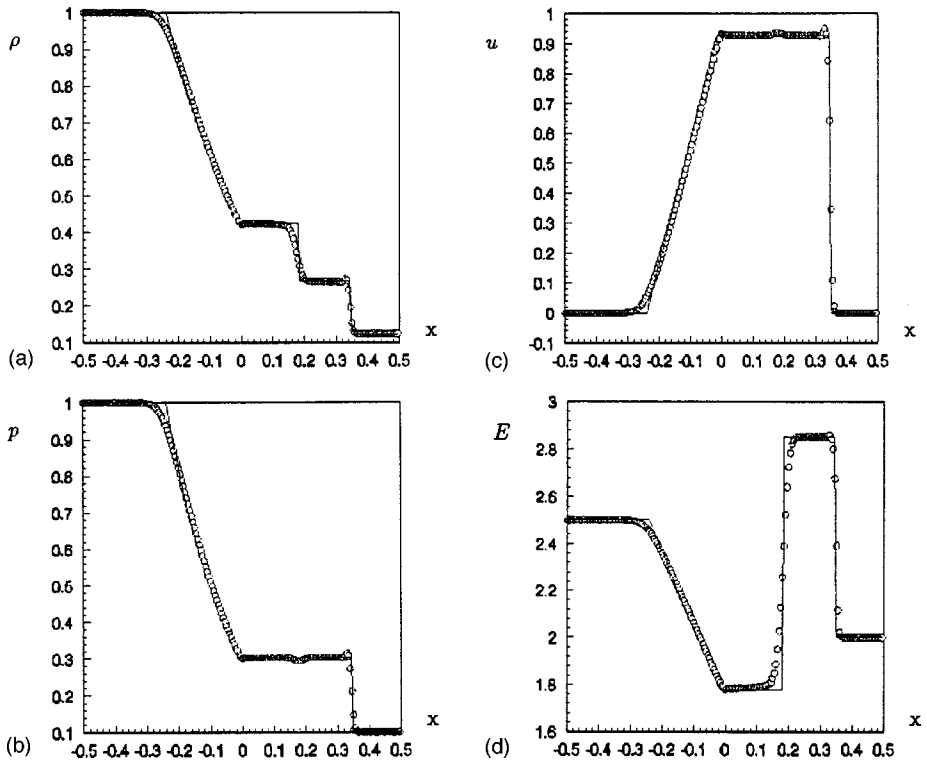

FIG. 2. Comparisons between numerical and theoretical results of Sod's test. Exact solution (line) and simulation (circles) of ρ, p, u, and E. Lattice size: 200×2. Output at 120 time steps. Parameters: $\gamma=1.4$; $c=3$; $\lambda=1.75$; $1/\tau=1.51$; $\varepsilon_A=2c^2$; $\varepsilon_B=0.6c^2$; $\varepsilon_D=0.13c^2$.

$$(\rho_R,u_R,p_R)=(1,1,1.8), \quad x>0.$$

The numerical results and exact solutions are shown in Fig. 4. The problem that should be mentioned is that two small tips emerge in the middle of the density and energy profiles. This unusual phenomenon also appeared in some high resolution schemes [14,15]. This is an interesting and difficult problem. We think this is because the relaxation factor τ and

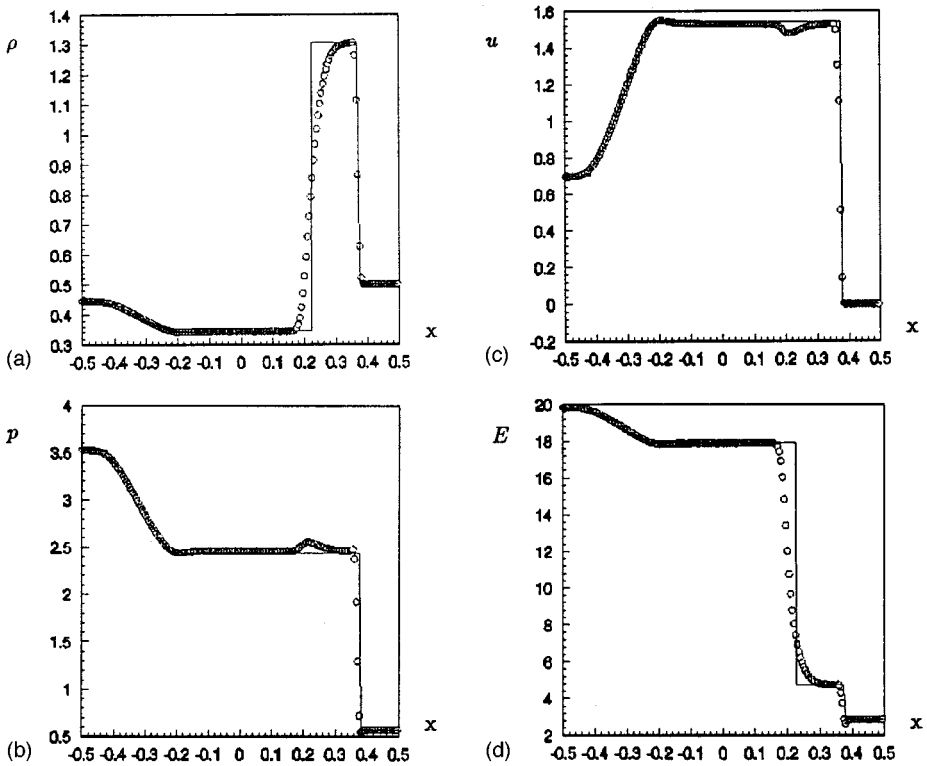

FIG. 3. Comparisons between numerical and theoretical results of Lax's test. Exact solution (line) and simulation (circles) of ρ, p, u, and E. Lattice size: 200×2. Output at 240 time steps. Parameters: $\gamma=1.4$; $c=8$; $\lambda=1.05$; $1/\tau=1.62$; $\varepsilon_A=2.5c^2$; $\varepsilon_B=0.6c^2$; $\varepsilon_D=0.13c^2$.

TABLE I. Riemann problems, L_1 norm errors. These results come from Ref. [13], except the LBM. Lattice size: $Nx=200$. The underlined results indicate the smallest L_1 norm error in every column.

	Sod's test $t=0.1644$			Lax's test $t=0.16$		
	Density	Velocity	Pressure	Density	Velocity	Pressure
LXF	0.017 69	0.028 14	0.015 82	0.061 65	0.055 57	0.065 37
LBM	0.008 04	0.016 73	0.007 92	0.030 51	0.019 37	0.049 01
ORD	0.005 78	0.009 59	0.004 60	0.022 31	0.017 09	0.019 95
ULT1	0.004 37	0.008 20	0.003 62	0.014 77	0.010 94	0.012 06
STG2	0.002 97	0.004 94	0.002 28	0.011 51	0.008 49	0.009 88
STGU	0.002 91	0.004 03	0.002 16	0.013 02	0.013 06	0.011 21
STGC	0.001 72	0.002 76	0.001 53	0.006 47	0.008 36	0.008 23
ULTC	0.003 61	0.008 04	0.003 62	0.008 72	0.010 74	0.011 83
Roe	0.008 36	0.011 45	0.006 66	0.028 27	0.021 92	0.026 55

time step Δt are unsuitable. In Roe's test, Δt may be so small that the distribution cannot reach equilibrium status. If we choose a large time step, the scheme is not stable. So the reason the tips emerge is that the Knudsen number becomes small.

Recently several sophisticated finite-difference techniques have been developed which are capable of capturing discontinuities more accurately. These include the essentially nonoscillatory (ENO) scheme [16] and the total variation diminishing (TVD) scheme and other high resolution schemes. TVD-type schemes have gained popularity for their applications in compressible flow. In TVD schemes the amount of this inherent numerical dissipation depends on the flux limiter user [17]. When these schemes are applied to shock tube problems, they produce very high resolution for the shock. The widths of shock waves are about one to two cells, the widths of contact discontinuity are about three to four cells. The numerical results from the LBM do not compare well with these high resolution schemes. If we combine the LBM with these high resolution techniques, the LBM would become a very interesting method.

IV. DISCUSSION AND CONCLUSIONS

We adopt the idea that the local equilibrium distribution satisfies conservation conditions and flux conditions of mass, momentum, and energy. This allows the dynamics equations of the perfect gas, especially the energy equation, to be easily recovered. In the model, the particle speed c should be chosen appropriately to meet the requirement of numerical sta-

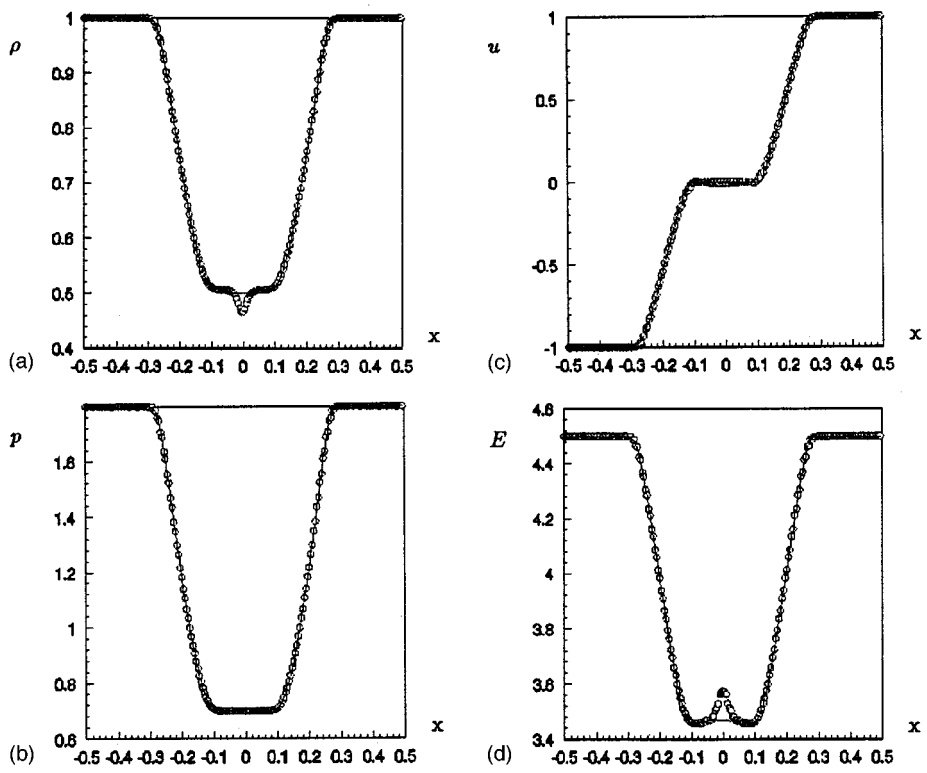

FIG. 4. Comparisons between numerical and theoretical results of Roe's test. Exact solution (line) and simulation (circles) of ρ, p, u, and E. Lattice size: 200×2. Output at 60 time steps. Parameters: $\gamma=1.4$; $c=3$; $\lambda=1.75$; $1/\tau=1.35$; $\varepsilon_A=2.0c^2$; $\varepsilon_B=0.6c^2$; $\varepsilon_D=0.13c^2$.

bility (such as the CFL condition [7,9]). On the other hand, to define total energy and internal energy for the recovery of the energy equation, the total energy in Refs. [18–20] is defined as the total kinetic energy of particles $E_T = \Sigma f_\alpha c^2/2$, which corresponds to $\varepsilon_A = \varepsilon_B = \frac{1}{2}c^2$, $\varepsilon_D = 0$ in our model. However, in a one or two speed model it causes two difficult problems: (i) it leads to $\gamma = 2$ (the so-called ideal case), (ii) the energy conservation can be derived from momentum flux conditions. To solve these problems, many researchers use a multispeed model (e.g., Refs. [18–20]) or introduce the concept of energy level (e.g., Ref. [21]). We utilize the merits of both of them. The present model is not only multispeed but also multienergy level. As a result, all equations of the perfect gas are successfully included in the lattice Boltzmann model, and the ratio γ of specific heats appears as a chosen parameter (the so-called general case). The remaining problems are those of accuracy and numerical stability [9]. The other advantage is that the pressure p (or internal energy E) in this model is a statistical quantity independent of ρ and ρu_i, so that a wide range of sound speed ($c_s = \sqrt{\gamma p/\rho}$) is allowable.

This square lattice has many spurious invariants in different time scales. We find the spurious invariants that relay on the moments of speed $\mathbf{e}_\alpha$. There are two types of invariants in our model: (i) In scale t_0, other equations are equivalent to Euler equations; (ii) there are some higher order moments, which may be spurious invariant, but the order is more than $O(\varepsilon)$.

Compared with the standard lattice Boltzmann model, our model has some new assumptions, for example, additional flux conditions, a three-energy-level assumption, parameter c being chosen freely. These assumptions cause the isothermal and low Mach limit to be removed, and the constraint of $\gamma = 2$ to be relaxed. At last, the simulation of aerodynamics with strong discontinuities is realized by using the lattice Boltzmann method. Although the model may not be a high resolution scheme, it is still attractive. This model preserves the main advantages of the available LBM model: noise-free, simple code and high parallelism, etc. The drawback of this model is that there are many parameters to be chosen and the result of Roe's test is not good enough.

ACKNOWLEDGMENTS

The authors are indebted to Professor Chen Shiyi, Professor Chen Hudong, Professor Qian Yuehong, Professor Zhao Kaihua, Professor Zhu Zhaoxuan, Professor Zhou Fuxin, and Professor Jin Xizhou for helpful discussions. This work was supported by the Laboratory for Nonlinear Mechanics of Continuous Media, Institute of Mechanics, Chinese Academy of Sciences, and by the National Natural Science Foundation of China under Grant No. 19372020.

[1] S. Y. Chen and G. D. Doolen, Annu. Rev. Fluid Mech. **30**, 329 (1998).
[2] Y. H. Qian *et al.*, Europhys. Lett. **17**, 479 (1992).
[3] H. D. Chen, S. Y. Chen, and M. H. Matthaeus, Phys. Rev. A **45**, 5339 (1992).
[4] F. J. Alexander *et al.*, Phys. Rev. A **46**, 1967 (1992).
[5] Y. H. Qian and S. A. Orzag, Europhys. Lett. **21**, 255 (1993).
[6] G. W. Yan, S. X. Hu, and W. P. Shi, Acta Scientiarum Naturalium Universitatis Jilinensis **1**, 1 (1997).
[7] S. X. Hu, G. W. Yan, and W. P. Shi, Acta Mech. Sin. **13**, 218 (1997).
[8] S. L. Hou *et al.*, J. Comput. Phys. **118**, 329 (1995).
[9] G. W. Yan *et al.* (unpublished).
[10] G. A. Sod, J. Comput. Phys. **27**, 1 (1978).
[11] P. D. Lax, Commun. Pure Appl. Math. **7**, 159 (1954).
[12] H. Nessyahu and E. Tadmor, J. Comput. Phys. **87**, 408 (1990).
[13] B. Einefldt *et al.*, J. Comput. Phys. **92**, 273 (1991).
[14] K. H. Prendergast and K. Xu, J. Comput. Phys. **109**, 53 (1993).
[15] K. Xu, J. Stat. Phys. **81**, 147 (1995).
[16] C. W. Shu and S. Oscher, J. Comput. Phys. **83**, 32 (1989).
[17] A. Harten, SIAM (Soc. Ind. Appl. Math.) J. Numer. Anal. **21**, 1 (1984).
[18] F. J. Alexander, S. Y. Chen, and J. D. Sterling, Phys. Rev. E **4**, 2249 (1993).
[19] G. R. McNamara, A. L. Garcia, and B. J. Alder, J. Stat. Phys. **27**, 395 (1995).
[20] Y. Chen, H. Ohashi, and M. Akiyama, J. Stat. Phys. **81**, 71 (1995).
[21] D. Bernardin, O. E. Sero-Guillaume, and C. H. Sun, Physica D **47**, 169 (1991).